

## Burner effects on melting process of regenerative aluminum melting furnace

Ji-min WANG<sup>1</sup>, Peng XU<sup>1</sup>, Hong-jie YAN<sup>2</sup>, Jie-min ZHOU<sup>2</sup>, Shi-xuan LI<sup>3</sup>, Guang-chen GUI<sup>3</sup>, Wen-ke LI<sup>1</sup>

1. School of Metallurgy and Resource, Anhui University of Technology, Maanshan 243002, China;

2. School of Energy Science and Engineering, Central South University, Changsha 410083, China;

3. Suzhou Longray Thermal Technology Co. Ltd., Suzhou 215008, China

Received 11 September 2012; accepted 29 February 2013

**Abstract:** According to the features of melting process of regenerative aluminum melting furnaces, a three-dimensional mathematical model with user-developed melting model, burner reversing and burning capacity model was established. The numerical simulation of melting process of a regenerative aluminum melting furnace was presented using hybrid programming method of FLUENT UDF and FLUENT scheme based on the heat balance test. Burner effects on melting process of aluminum melting furnaces were investigated by taking optimization regulations into account. The change rules of melting time on influence factors are achieved. Melting time decreases with swirl number, vertical angle of burner, air preheated temperature or natural gas flow; melting time firstly decreases with horizontal angle between burners or air-fuel ratio, then increases; melting time increases with the height of burner.

**Key words:** regenerative aluminum melting furnace; burner; melting process; numerical simulation; multi-element non-linear regression

### 1 Introduction

Aluminum and its alloys are widely used in the economy, particularly in the transportation, packaging and construction industries. Most aluminum melting is accomplished in large, natural-gas-fired furnaces. Although much effort has been made to improve energy efficiency in melting process, current energy efficiency in most reverb furnaces is still low. An understanding of the fundamentals and interactions of flow and heat transfer in the furnace plays key roles in improving energy use, increasing production rate, and reducing pollutant formation.

LI et al [1] put forward the energy availability concept to analyze the maximum energy efficiency and the minimum flue gas heat loss in aluminum reverb furnaces. Methods that can improve the energy efficiency and reduce the pollutant emissions from the melting operations were also addressed. GOLCHERT et al [2] detailed a systematic computational fluid dynamics

(CFD) study on how the variability of the nitrogen concentration coupled with partial replacement of air with pure oxygen affects heat transfer and pollutant formation in aluminum melting furnaces. WILLIAMS et al [3] developed a method of determining the transient heat transfer efficiency throughout the furnace cycle and took advantage of this knowledge to optimize the melting procedure through furnace controls and proper production operations. To increase the furnace productivity and reduce the fuel consumption, LAZIC et al [4] applied measuring technique and thermodynamics analysis to the combustion process of aluminum melting furnaces. KUMAR et al [5] and GOLCHERT et al [6] established a computational model with the burden at a particular stage of the melting process to understand the effect of the flame interaction with unmelted aluminum. Through scale modeling and verifiable computational results, “improving energy efficiency in aluminum melting” project team funded by the U.S. Department of Energy [7–10] built a 2000 pounds experimental reverb furnace and gave some background into the

**Foundation item:** Project (2009bsxt022) supported by the Dissertation Innovation Foundation of Central South University, China; Project (07JJ4016) supported by Natural Science Foundation of Hunan Province, China; Project (U0937604) supported by the National Natural Science Foundation of China

**Corresponding author:** Ji-min WANG; Tel: +86-13965384801; E-mail: [endlessfree@163.com](mailto:endlessfree@163.com)

DOI: 10.1016/S1003-6326(13)62843-5

computational aspect, analyzed the influence of power input, burner loading and combustion space volume on melting efficiency, performed parametric studies to optimize operation in industrial furnaces, and indicated that the computations are useful and identified future areas of research. BELT [11] pointed out that the largest improvement of energy efficiency is reduction in burner fire rate. The next most effective improvement is the reduction of excess air and an idle mode. Reduction of flue temperatures and use of the pilot relight option also increases efficiency. To find relationships among firing rate, heat absorption rate, melting rate, and energy efficiency in aluminum melting and to predict the optimum operating conditions where the maximum energy efficiency can be achieved, LI et al [12] developed the modified Essenhigh/Tsai furnace model applied to aluminum melting furnaces based on two main assumptions. To verify that the results from experiments conducted in an experimental research furnace is validate for the operations of industrial furnaces, PENMETS A et al [13] developed appropriate scale laws with the partial scaling relaxation for aluminum melting furnaces, and conducted model experiments on the thermal conduction loss across furnace walls. NIECKELE et al [14–18] analyzed combustion process of aluminum melting furnaces with pure oxygen and air as the oxidant, liquid oil and natural gas as the fuel, various oxygen injection configuration, and different combustion methods. CLARK [19] employed a laboratory scale reverb to discuss the interaction between aluminum, refectories, and the melt atmosphere. STEVENS and FORTIN [20] described accurately the phenomena observed in industrial scale melt furnaces using the pilot scale top-charge.

Computational simulations have the obvious advantage over experimentation in what they can be performed cheaply and quickly, allowing for a parameter regime to be investigated prior to capital outlay on an industrial furnace. Nevertheless, most literature about numerical simulation of aluminum melting furnaces did not consider the molten aluminum in the furnace and the interaction between combustion space and aluminum bath. As a result, the important information in the molten aluminum has not been acquired yet. Hence, in the present work, by taking into account heat transfer between combustion space and aluminum bath, phase change, burner reversing and changing burning capacity, a three dimensional mathematical model was established. Melting process of regenerative aluminum melting furnace was simulated numerically with user-developed model in CFD framework. To understand the intricate interactions of geometric and operational characteristics of reverb furnaces, the effects of the various combinations of system parameters which include burner

placement, structure and loading on melting process were discussed. It yields a clear and concise means of looking at furnace performance, yielding new insight into the practical operation and retrofit of the furnace and indicating the potential for new control algorithms.

## 2 Physical model

Many aluminum reverb furnaces are basically rectangular boxes. However, there exist several round furnaces in the industry whose operation is slightly more different than the common rectangular holding furnaces. These round tops have removable roof that can be flat or curved. The roof is mechanically removed from the furnace and the unmelted scrap is lowered into the furnace. To avoid any proprietary issues, a ‘generic’ aluminum melting furnace was adopted. This furnace has two burners located on the side wall with the secondary flue located between the two burners. This is an industry ‘standard’ for melting furnaces. The heat input is provided by natural gas in a combustion chamber. Heat is transferred from the hot combustion flue gases to the molten aluminum surface in the combustion chamber. In the upper part of the furnace, natural gas is mixed and burnt with air. Meanwhile, in the lower part of the furnace solid aluminum is melted and liquid metal is heated to the specified bath bulk temperature. When the furnace is in operation, aluminum loads are alternatively heated by regenerative burners. These burners have slightly injection angle to avoid direct impingement upon the unmelted aluminum. The height of the secondary flue is a little more than that of burners. Once in the furnace, the aluminum scrap is first heated up, then alloyed and treated, and finally transferred to holding furnaces for casting into large ingots or for other processes. The geometry schematic of the furnace is shown in Fig. 1. By the way, the furnace linings and flue are not included. Taking geometry structure of the burner in the furnace in consideration, swirling jet was generated by volute swirler. The calculation formula of swirl number ( $s$ ) in considering the influence of center tube is

$$S = 2 \frac{(d_2^2 - d_1^2)l}{WHd_2} \quad (1)$$

where  $d_1$  and  $d_2$  are the inner diameter and outer diameter, respectively;  $W$  and  $H$  are the length and width of inlet cross section, respectively;  $l$  is the offset distance.

In the present study, some assumptions are made to simplify the physical model.

1) According to the features of melting process, the liquid aluminum can be assumed to be stagnant. Chemical reactions above the melt surface can be neglected. Radiation and convection between combustion space and aluminum bath are only taken into account.

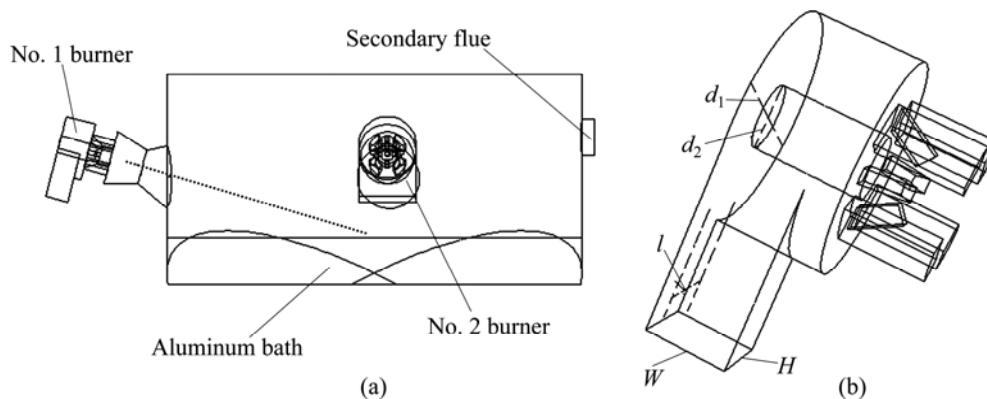


**Fig. 1** Geometry schematic of regenerative aluminum melting furnace: (a) Regenerative aluminum melting furnace; (b) Volute swirler

2) Melt surface is homogeneously covered by alumina [14]. The thickness and the emissivity of oxide layer are 5 mm and 0.33, respectively.

3) The heat loss is neglected by the walls [21]. The emissivity of the inner walls is supposed to be 0.8.

4) Liquid flow after solid melting is not included in the model. The latent heat in the solid–liquid zone is assumed to release linearly.

5) However, after the solid aluminum is melted, heat requirement of molten aluminum reduces substantially, and aluminum temperature increases quickly. Thus, heat supply is adjusted to prevent molten aluminum from overheating. During the melting process, both natural gas mass flow and air velocity vary with melting time. To solve conveniently, it may be supposed that there is a stepwise relationship between burning capacity and liquid fraction. Here, the burning capacity is a correction factor for natural gas mass flow and air velocity.

6) Considering working principles and characteristics of regenerative burners, melting process is seen as an unsteady state. The reversing time is 60 s.

7) The absorption coefficient is assumed to comply with the Weighted Sum of Gray Gases Model. The composition of natural gas is supposed to be standard.

### 3 Computational models and solution

A general-purpose finite volume based user-defined model in CFD framework is used in this study. The code solves for the mass, momentum, species and energy conservation equations with appropriate sub-models for simulating the underlying complex physics, such as turbulence, combustion, radiation, melting.

Reynolds Averaged Navier-Stokes is a well established approach for modeling turbulence in complex industrial systems. The standard k-epsilon model was

used to model viscous effect. In a combustion simulation, it is necessary to predict the major species fields including the reactants as well as the major combustion products as prescribed by the reaction mechanism. Moreover, in turbulent conditions the turbulence-chemistry coupling must be modeled. In this work, the former phenomenon is simulated using multi-species transport model with volumetric reactions, while the latter is simulated using the eddy dissipation model, which assumes that the volumetric reaction rate is based on the turbulent mixing. A major advantage of the eddy-dissipation model is that it is equally applicable to non-premixed flames, as well as premixed flames. Radiation is one of the dominant modes of heat transfer in a furnace and its inclusion in the model is necessary to calculate the temperature fields accurately. Radiation transport, apart from being spatially varying, is also direction dependent and the presence of greenhouse gases, such as  $\text{CO}_2$  and  $\text{H}_2\text{O}$ , can make the medium participate in the radiative transport. These complexities make the radiation modeling non-trivial. In the present work, P-1 model is used to solve the radiation transfer equation. The standard wall functions are used to treat the flow in the near-wall region.

According to the assumption 1), in the current model, the aluminum bath is regarded as a conducting solid. Most of the heat is transferred by radiation instead of convection in an aluminum melting furnace. The basis for radiant heat transfer is Stefan-Boltzman equation. Although radiation accounts for most of the heat transfer, convection cannot be ignored. Convection heat transfer is normally expected to be 5% to 10% of radiant transfer depending on the furnace temperature, combustion conditions and burner arrangement. The total heat transfer to the bath is the sum of the radiant and convective heat transfer through the interface of fluid and solid:

$$\lambda \frac{\partial T}{\partial n} \Big|_w = h(T_f - T_w) + \varepsilon \sigma (T_f^4 - T_w^4) \quad (2)$$

where  $\lambda$  is the thermal conductivity of the solid;  $h$  is the local convective heat transfer coefficient;  $T_f$  is the fluid temperature;  $T_w$  is the temperature of the coupled wall;  $\varepsilon$  is the solid emissivity;  $\sigma$  is the Stefan-Boltzmann constant.

Melting process of aluminum melting furnaces involves phase change of aluminum melting, which is accomplished by melting sub model. To deal with the latent heat term, the key is to obtain the relationship between liquid fraction and temperature. The equivalent-specific heat method is chosen to process the latent source item of phase change [22]. Because conduction in phase region is affected not only by the latent heat, but also by the change of the physical characteristics due to composition change, the physical properties of melting process are defined according to Ref. [23].

$$c(T) = \begin{cases} c_1(T), & T \leq T_S \\ [c_1(T) + c_2(T)]/2 + L/(T_L - T_S), & T_S < T < T_L \\ c_2(T), & T \geq T_L \end{cases} \quad (3)$$

where  $c_1$  is the specific heat of the solid aluminum;  $c_2$  is the specific heat of the liquid aluminum;  $T_S$  is the solidus temperature;  $T_L$  is the liquidus temperature;  $L$  is the latent heat.

In this study, according to the assumptions 5) and 6), the changes of burning capacity and burner reversing are implemented by user-developed burning capacity and burner reversing sub model. Among above models, the burning capacity and burner reversing model are coupled with the melting model by liquid fraction to alter natural gas mass flow and air velocity and set boundary conditions. In Ref. [24], the governing equations and how the numerical model is established are described, and how the hybrid programming method is conducted in the model is also given.

The initial temperature of aluminum scrap is set to be 300 K. Mass flow, temperature and hydraulic diameter of air inlet are set to be 1.879 kg/s, 773 K, and 475 mm, respectively. Velocity, temperature and hydraulic diameter of natural gas inlet separately are set to be 45.355 m/s, 300 K, and 64 mm, respectively. Turbulence intensities of air inlet and natural gas inlet are 3.78% and 3.23%, respectively. The main flue and secondary flue are set to outflow, and the weights are 0.8 and 0.2, respectively.

The mesh distribution was generated with the FLUENT auxiliary tool GAMBIT. A fine mesh is needed to define inlet region at the burners of small dimension. Considering computing resource and accuracy of results, mesh independence test and time-step independence test have been undertaken. When the relative error of furnace

temperature is less than 5%, grid spacing and time step have no influence on the simulation results. Five combinations of grid and time-step sizes are compared with the total number of cells varying from 202, 346 to 455, 353 and the time-step size ranging from 0.5 to 10 s. Thus, from Fig. 2, a total of 377, 442 cells and a time-step size of 1 s are adopted in the present study.

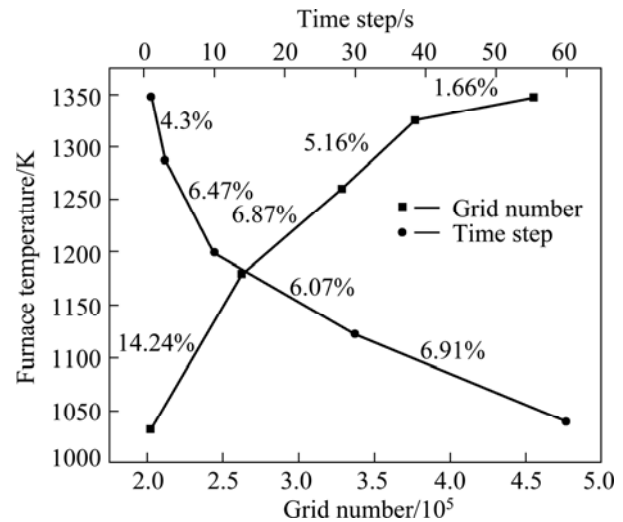


Fig. 2 Grid number and time step independence test

#### 4 Experimental measurement and model validation

Heat balance test of a 35 t aluminum melting furnace operating under the reference operation condition was investigated experimentally. Here, a brief introduction of the experimental study was given. The furnace was treated as the objective during heat balance test. Throughout the whole operation period, i.e., from aluminum scrap charging to product holding, parameters including temperature of combustion chamber, melt temperature, and flue gas flow rate in the duct were measured and recorded continuously. In addition, fuel-mixture flow rate and duration of melting process were recorded as well. Based on these data, heat balance calculation can be performed according to the relevant national standard. Accordingly, details of the energy flow of the furnace were estimated, by which primary operation parameters for the furnace can be obtained.

Simulation results must be confirmed by in-situ measurement. In the present study, according to on-the-spot application status, CFD model validation was performed using the comparison of aluminum temperature and furnace temperature between computational data and measured data, as shown in Fig. 3. The experimental conditions were reported in Ref. [24]. The measured position of furnace temperature was 2900 mm away from the melt surface, and 400 mm away

from the inner wall. The location of the test points of aluminum temperature lied on 500 mm away from slag-off doors, and 230 mm away from the melt surface. The temperature was measured by means of thermocouple NiCr–Ni and the major gas-phase species concentrations were detected by flue gas analyzer from Testo in one point at the end of the furnace chamber, where the waste gases entered the flue. Combustion product samples were taken using a stainless steel probe. The furnace pressure is usually at heart level. The results are listed Table 1. The relative error between them is less than 10%. It is important to keep in mind the fundamental differences between an experimental furnace and a computer model. Considering these assumptions, the trend of simulation results is in accordance with that of the measured data. Thus, the computational models were proven to be reliable and accurate. The results show that melting phenomenon of the furnace may be revealed thoroughly. It is also indicated that the optimization of parameters for aluminum melting furnaces may be studied by the above model.

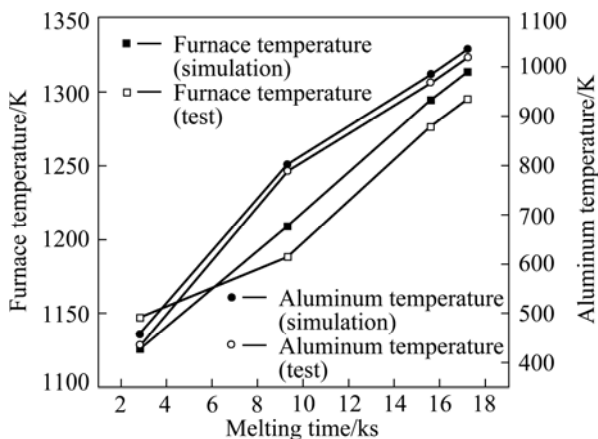


Fig. 3 Comparison of temperature between computational data and test data in combustion space and aluminum bath

### 5 Optimization regulations and simulation conditions

As combustion gases inside the furnace rotate, it may enhance fuel–air mixing, and the residence time of exhausted gas is prolonged, which results in furnace temperature increase, and makes the temperature homogeneous. Swirl number is the major similarity norm

of swirling jet. The swirl number is an indication of the intensity of swirl flow. It is usually defined as the ratio of tangential to axial momentum. The critical swirl intensity is 0.6. Rotating flow in aluminum melting furnaces is achieved by changing swirl number or horizontal angle between burners. Optimization regulations are listed as follows.

1) Melting time is as short as possible, and both RSD of aluminum temperature and RSD of furnace temperature should be also small [25–27].

2) Flue gas temperature must be high enough, but the flue gas temperature never exceeds 1423 K [28].

3) Furnace pressure is a little positive, 10–20 Pa [27,28]. If the pressure difference between the furnace chamber and surroundings is not correct, a great leakage of hot gases from the furnace or infiltration of cold air into the chamber will occur.

4) Aluminum melting furnaces work in micro-oxidation atmosphere, which may make natural gas burn completely, and reduce the heat of the exit flue gas. Thus, oxygen concentration in flue gas is less than 3% [28,29].

Using the above mathematical model, swirl number  $S$ , horizontal angle between burners  $\alpha$ , height of burner  $H$ , vertical angle of burner  $\theta$ , air-to-fuel mass ratio  $n$ , air preheated temperature  $T$ , natural gas mass flow  $M$  were selected as influence factors on melting process of regenerative aluminum melting furnaces. The effects of the factors on the performance of aluminum melting furnaces were investigated. The conditions of numerical simulation are shown in Table 2. A base case under consideration in the body of Table 2 is marked in an underline. Here, different swirl number is obtained by changing the size of volute swirler such as the cross-section dimension and offset distance. The size of volute swirler for different swirl number is shown in Table 3 with a wide range of swirl number  $S=0-1.1375$  to cover three regimes: non-swirling jet with  $S=0$ ; weakly swirling jets in the range of  $0 < S < S_c=0.6$ ; strongly swirling jets for  $S > S_c=0.6$ .

The quality of temperature distribution is measured by relative standard deviation (RSD), which can be expressed as

$$RSD = \sigma / \bar{x} \tag{4}$$

where  $\sigma$  is the standard deviation;  $\bar{x}$  is the mean value. Thus, RSD of aluminum temperature and RSD of furnace temperature are easily defined.

Table 1 Comparison of simulation results and test values for aluminum melting furnace

Item	Melting time/h	$\varphi(\text{CO}_2)/\%$	$\varphi(\text{H}_2\text{O})/\%$	$\varphi(\text{N}_2)/\%$	$\varphi(\text{O}_2)/\%$	$\varphi(\text{NO}_x)/10^{-6}$	Pressure/Pa	Aluminum temperature/K	Furnace temperature/K
Measurement value	5.1	3.12	5.97	76.53	14.34	400	18	1021	1280
Simulation result	4.8	3	5.75	76.68	14.53	415	16.51	1035	1337
Relative error/%	5.88	3.85	3.67	0.20	1.32	3.75	8.28	1.37	4.35

**Table 2** Conditions of numerical simulation

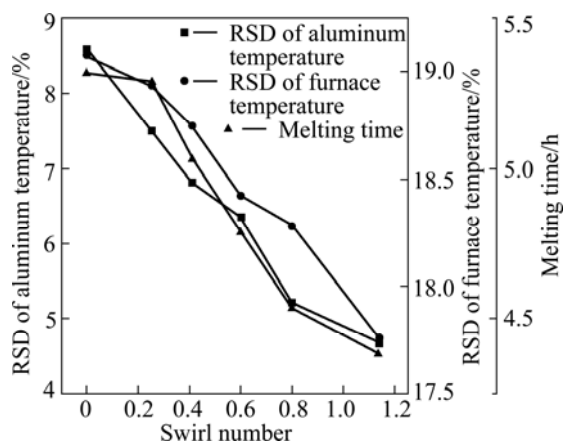
$S$	$\alpha/(\circ)$	$H/\text{mm}$	$\theta/(\circ)$	$n$	$T/^\circ\text{C}$	$M/(\text{m}^3\cdot\text{h}^{-1})$
0	60	1407	11	1.05	250	400
0.2528	75	1507	13	1.1	350	450
0.41	90	1607	15	1.15	450	500
0.6	105	1707	17	1.2	550	550
0.8	120	1807	19	1.25	650	600
1.1375						

**Table 3** Size of volute swirler for different swirl number

Swirl number, $S$	Cross-section dimension, $W\times H/\text{mm}$	Offset distance, $l/\text{mm}$	Outer diameter, $d_1/\text{mm}$	Inner diameter, $d_2/\text{mm}$
0	320×790	0		
0.2528	300×300	250		
0.41	260×240	280		
0.6	227.5×200	300	800	240
0.8	230×160	320		
1.1375	280×100	350		

## 6 Burner effects on melting process of regenerative aluminum melting furnace

Figure 4 presents change curves of the RSD of aluminum temperature, melting time and RSD of furnace temperature with the swirl number. If the swirl intensity is high, the flow swirls strongly, enlarging the expanding angle as well as the recirculation zone. The amount of hot gas recirculating at the root of the flame also increases. This enhances the turbulent diffusion and, therefore, the early mixing. As the swirl number increases, heat transfer between combustion space and aluminum bath was strengthened. And it also improves the heat transfer between combustion gases. Thus, both the RSD of aluminum temperature and RSD of furnace

**Fig. 4** Change curves of RSD of aluminum temperature, RSD of furnace temperature and melting time with swirl number

temperature decrease with the swirl number, yet the furnace temperature increases with the swirl number. Since the furnace temperature increases and gas disturbance enhances, radiant heat transfer and convection heat transfer between combustion gases and aluminum loads are promoted, which leads to the melting time to reduce with the swirl number. In particular, the melting time has a marked impact on hydrogen reaction and oxidation of the molten aluminum. Therefore, the increase of the swirl number may reduce oxidation burning loss and absorbed hydrogen content. It may save the energy and resource and improve the product quality.

Figure 5 shows temperature field and streamline of different swirl number inside the furnace. When the swirl number is greater than 0, a large eddy appears far way the main flue in the furnace, which is the main cause of the changing trend in Fig. 4. For high swirl number may promote mixing and burning of gases, the maximum temperature of the flame decreases with the swirl number, but furnace temperature is higher and more uniform.

Change curves of the RSD of aluminum temperature, melting time and RSD of furnace temperature with the horizontal angle between burners are shown in Fig. 6. When the horizontal angle between burners is less than  $90^\circ$ , the combustion gases in the furnace rotate clockwise. The lower temperature zones locate at aluminum loads between burners. This is the reason that aluminum loads in the zones always exchange heat with lower temperature gases. However, when the horizontal angle is greater than  $90^\circ$ , the combustion gases in the furnace rotate counter-clockwise. As a result, the aluminum loads are alternatively heated by regenerative burners, which makes melt temperature more homogeneous. The residence time is critical to furnace operation. The longer the combustion gases reside in the furnace, the higher the probability that the energy is radiated to the aluminum. When the horizontal angle between is greater than  $90^\circ$ , most of exhaust gases directly flow out from the main flue. Thus, the residence time of gases in the furnace is reduced, which weakens heat transfer between combustion gases, so the RSD of furnace temperature increases with the horizontal angle between burners. It is seen from Fig. 7 that the flame slightly shifts to the main flue when the horizontal angle is greater than  $90^\circ$ . High-temperature flue gas is discharged from the main flue, which reduces heat transfer between flue gas and aluminum loads. Therefore, the melting time is a little longer. Additionally, when the horizontal angle between burners is less than  $90^\circ$ , the flame directs to the side wall. Although it strengthens radiation heat transfer between combustion space and aluminum bath, radiation heat transfer is limited due to the smaller emissivity of pure aluminum, and it reduces

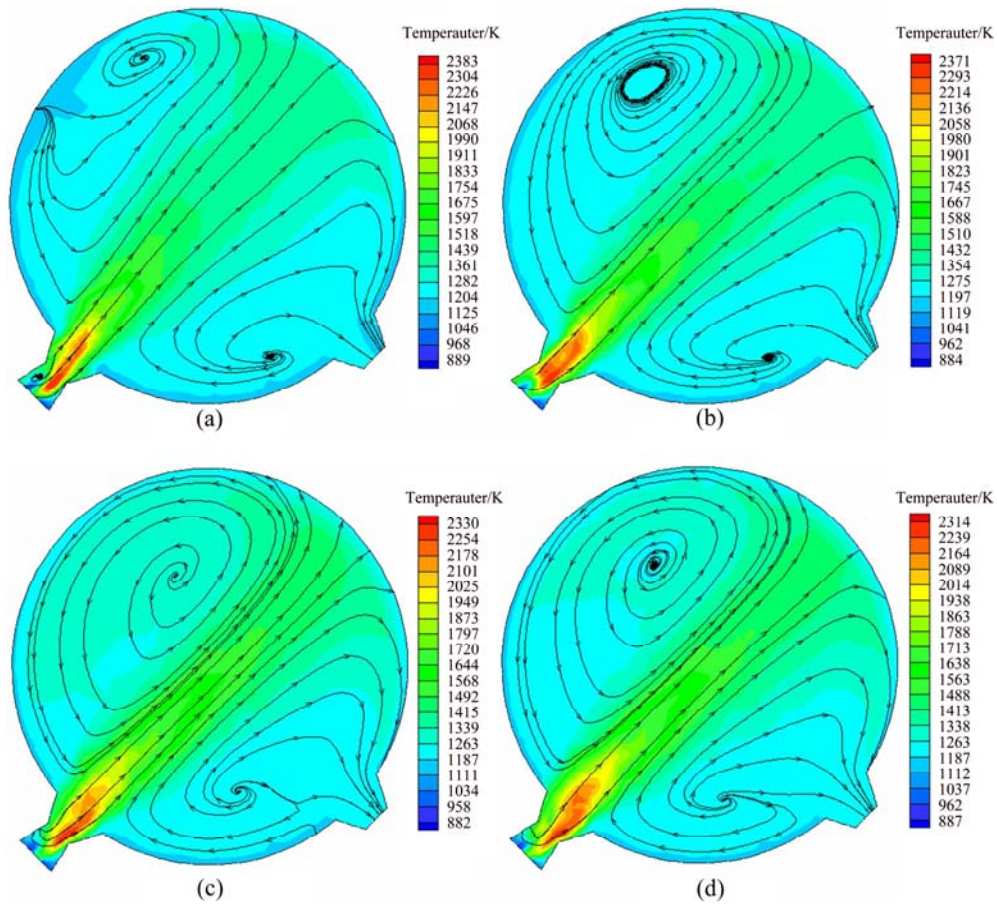


Fig. 5 Temperature field and streamline for combustion space on different swirl number: (a)  $S=0$ ; (b)  $S<0.6$ ; (c)  $S=0.6$ ; (d)  $S>0.6$

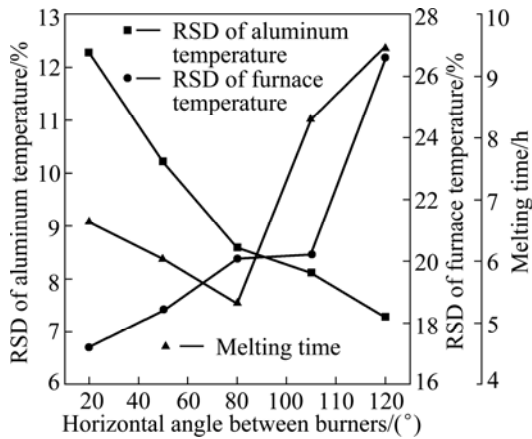


Fig. 6 Change curves of RSD of aluminum temperature, RSD of furnace temperature and melting time with horizontal angle between burners

convective heat transfer between combustion gases and aluminum loads, and enhances the undesirable heat loss through the walls in which gas flow directly impinges on the opposite wall. Therefore, the melting time is longer.

Figure 7 plots temperature contours and streamline of different horizontal angle between burners. The brighter the color in the picture, the higher the gas temperature. As can be seen in Fig. 7, combustion gases

in the furnace rotate clockwise or counter-clockwise when the horizontal angle between burners is greater or less than  $90^\circ$ , which makes furnace temperature increase or decrease. Besides, when the combustion gases in the furnace rotate counter-clockwise, the flame injects towards the main flue. Therefore, if the velocity of gas flow is too small, it is easy to cause “short-circuit” of the flame.

Figure 8 shows change curves of the RSD of aluminum temperature, melting time and RSD of furnace temperature with the height of burner. Increased height of burner reduces the gas velocity above melt surface, which makes velocity profile above melt surface more even, so it reduces the RSD of aluminum temperature. When the height of burner is too high, high-temperature zones of the flame concentrate in the upper part of the chamber, which brings about inhomogeneous furnace temperature. As the height of burner decreases, the flame slow moves towards melt surface. The temperature distribution has a tendency to be even, yet when the height of burner is too low, high-temperature zones of the flame locate at the lower part of the chamber, which arises furnace temperature more uneven. The RSD of furnace temperature firstly decreases with the height of burner, then increases, finally increases again.

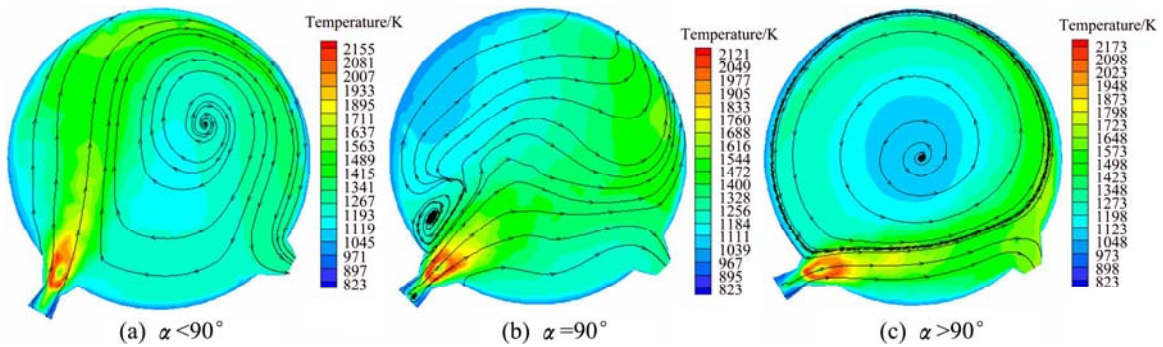


Fig. 7 Temperature field and streamline for combustion space on different horizontal angle between burners

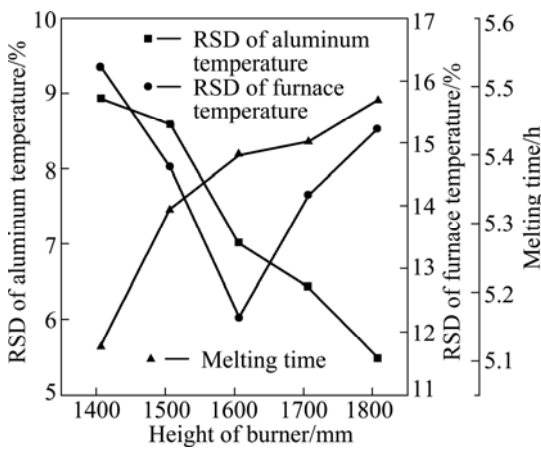


Fig. 8 Change curves of RSD of aluminum temperature, RSD of furnace temperature and melting time with height of burner

As the height of burner rises, convective heat transfer between combustion gases and aluminum loads reduces, which extends the melting time.

Figure 9 shows the change curves of the RSD of aluminum temperature, melting time and RSD of furnace temperature with the vertical angle of burner. As the vertical angle of burner elevates, the gas velocity above melt surface increases, and the uniformity of gas velocity above melt surface increases. Because melt temperature distribution is determined by gas velocity distribution above melt surface, the RSD of aluminum increases with the vertical angle of burner. When the vertical angle of burner is too large, high-temperature zones of the flame approach to the burners, which results in inhomogeneous furnace temperature. As the vertical angle of burner decreases, the flame slow moves towards melt surface and the hearth fullness is improved. The temperature distribution tends to be even, yet when the vertical angle of burner is too small, high-temperature regions of the flame locate at the upper part of the chamber, which gives rise to furnace temperature more uneven. All in all, the RSD of furnace temperature firstly decreases with the vertical angle of burner, then increases. With increasing vertical angle of burner, gas velocity above melt surface

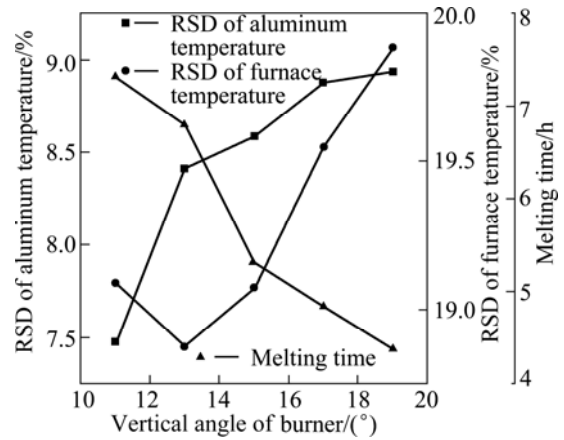
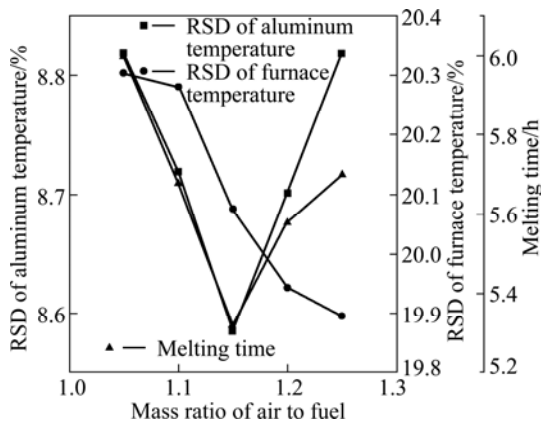


Fig. 9 Change curves of RSD of aluminum temperature, RSD of furnace temperature and melting time with vertical angle of burner

increases, this enhances the convective heat transfer between combustion gases and aluminum loads. Therefore, this means a decrease in the melting time.

Change curves of the RSD of aluminum temperature, melting time and RSD of furnace temperature with the mass ratio of air to fuel are plotted in Fig. 10. As the mass ratio of air to fuel increases, after air combusts with natural gas, the excess air promotes combustion gases mixing and heat transfer between low temperature air and high-temperature flue gas, which reduces the RSD of furnace temperature. There is an increasing trend of air mass flow with the increase of the air-to-fuel mass ratio. Therefore, the velocity of air inlet increases, which provides better combustion gases mixed. Gas velocity distribution above melt surface becomes even. Thus, the RSD of aluminum temperature decreases. On the other hand, if air mass flow is too large, there is too much cold air in the furnace, which increases the RSD of aluminum temperature. With the increase of the air-to-fuel mass ratio, high-temperature flue gas increases, which strengthens heat transfer between combustion gases and aluminum loads, hence the melting time reduces. If the mass ratio of air to fuel is too

large, excess cold air needs to absorb heat. What's more, these higher velocities reduce the retention time of the hot gases in the furnace and thus reduce the probability of these gases radiating their energy to the loads. As a result, the melting time increases again. Furthermore, the excess air increases mass flow rate of the combustion products, leaving the furnace chamber, so the energy carried out in the waste gases is thus increased. It is also expected that these higher velocities will lead to a less efficient operation. In short, the melting time firstly decreases with mass ratio of air to fuel, then increases.



**Fig. 10** Change curves of RSD of aluminum temperature, RSD of furnace temperature and melting time with mass ratio of air to fuel

Figure 11 illustrates the change curves of the RSD of aluminum temperature, melting time and RSD of furnace temperature with the air preheated temperature. It is observed that the activation energy of premixed gases increases as the air preheated temperature increases. As a consequence, much energy can be released. Besides, the preheated air brings heat by itself. The rise of furnace temperature is obvious. However, it increases the RSD of furnace temperature. Meanwhile, the RSD of aluminum

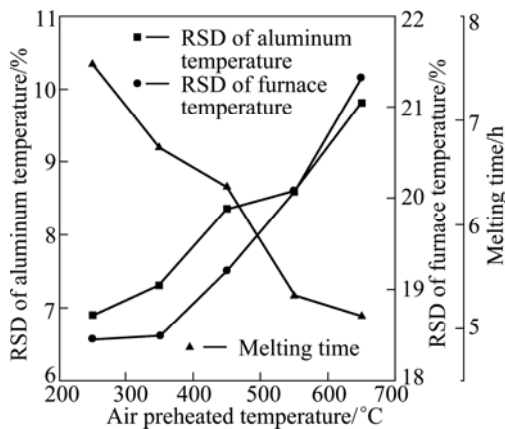


**Fig. 11** Change curves of RSD of aluminum temperature, RSD of furnace temperature and melting time with air preheated temperature

temperature increases. Higher air preheated temperature causes more intensive heat transfer from combustion gas to aluminum loads. Consequently, the melting rate is increased.

Change curves of the RSD of aluminum temperature, melting time and RSD of furnace temperature with the natural gas mass flow are shown in Fig. 12. The increase of natural gas mass flow enhances the gas flow velocity and turbulent intensity in the furnace. Therefore, heat flux caused by convection increases, that is, more heat is transferred into the metal layer. The RSD of furnace temperature decreases, and it cuts down the melting time accordingly. As the natural gas mass flow increases, gas velocity distribution above melt surface is more uneven. In addition, it leads to be greatly different in temperature between the upper and the bottom of aluminum due to high flame temperature near melt surface.

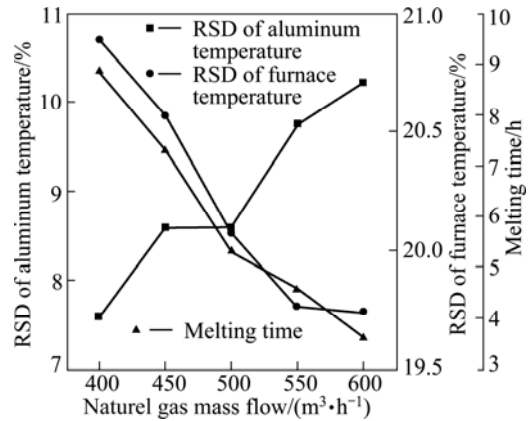


**Fig. 12** Change curves of RSD of aluminum temperature, RSD of furnace temperature and melting time with natural gas mass flow

By the analysis of preliminary simulation results, furnace pressure, flue gas temperature, and oxygen concentration in flue gas correspond with optimization regulations. According to the analysis of heat balance test, the heat loss of flue gas is reduced through decreasing melting time, which improves heat efficiency of the furnace. On the other hand, it makes aluminum load quickly. However, to avoid overheating molten aluminum, RSD of aluminum temperature should be smaller. Therefore, in order to optimize melting process of regenerative aluminum melting furnaces, RSD of aluminum temperature ( $Y_1$ ), melting time ( $Y_2$ ) and RSD of furnace temperature ( $Y_3$ ) were designed for evaluation criteria. Based on the simulation results, the relationship between evaluation criteria and factors is obtained by fitting the data.

It is indicated that the relationship between the RSD of aluminum temperature and air-to-fuel mass ratio is not monotonic. The melting time is not linear with the change of horizontal angle between burners or air-to-fuel

mass ratio. As the vertical angle of burner, height of burner or air preheated temperature increases, the RSD of furnace temperature obeys a quadratic function. Therefore, when all them were taken into account, by multi-element non-linear regression on the basis of the simulation results, the empirical correlations for the RSD of aluminum temperature ( $Y1$ ), melting time ( $Y2$ ) and RSD of furnace temperature ( $Y3$ ) are obtained as follows:

$$\begin{cases} Y1 = 24.592\theta^{0.296} H^{-2.199} S^{-0.42} \alpha^{-0.8} \cdot \\ T^{0.341} M^{0.743} (n+195.676)^{2.024} \\ Y2 = 88.045\theta^{-0.893} H^{0.284} S^{-1.987} \alpha^{0.971} \cdot \\ (\alpha + 0.63n + 32.083)^{0.668} T^{-0.346} M^{-1.286} n^{0.325} \\ Y3 = 8.94\theta^{-0.29} (\theta - 0.113H + 0.207T + 174.003)^{3.401} \cdot \\ H^{3.471} S^{-0.007} \alpha^{0.639} T^{-2.676} M^{-0.184} n^{-151} \end{cases} \quad (5)$$

The relationship between the evaluation criteria and factors accords with the influence analysis of burners on melting process of regenerative aluminum melting furnaces, as show in Fig. 13. The closer the coefficient ( $R^2$ ) is to unity, the better the empirical model fits the actual data. The coefficients of determination were calculated as 0.9568, 0.9715 and 0.9771 for the RSD of aluminum temperature, RSD of furnace temperature and melting time, respectively, indicating good agreement between the experimental results and predicted values. Using Eq. (5), the relative error between predicted values and simulation results varies from  $-12.5\%$  to  $8.94\%$ ,  $-15\%$  to  $16.27\%$ ,  $-6.48\%$  to  $11.24\%$  for the RSD of aluminum temperature ( $Y1$ ), melting time ( $Y2$ ) and RSD of furnace temperature ( $Y3$ ), respectively, suggesting that the regressive formula were proved to be reliable and accurate, particularly the relationship between melting time and vertical angle of burner is also in agreement with Ref. [10]. It is seen from Table 4 and Eq. 5 that the relationship between evaluation criteria and factor is non-linear. Therefore, in such multivariate problems, use of non-linear technique like Taguchi method, response surface methodology or genetic algorithm is suitable to employ for parameter optimization of melting process of aluminum melting furnaces.

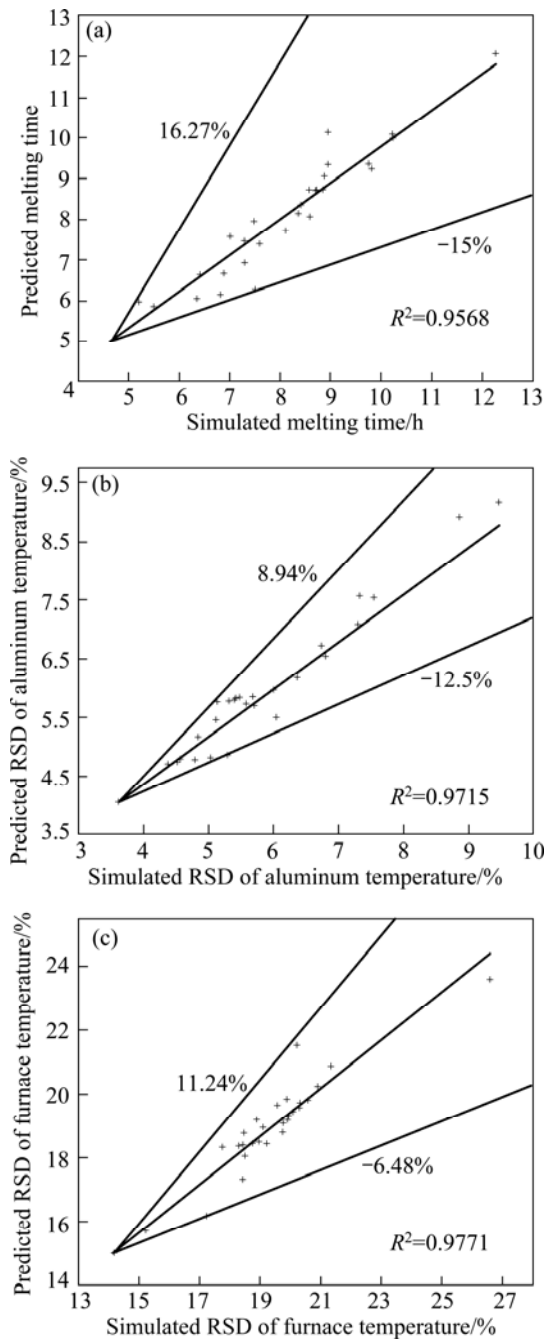


**Fig. 13** Comparison of simulation results and predicted values for evaluation criteria: (a) Melting time; (b) RSD of aluminum temperature; (c) RSD of furnace temperature

**Table 4** Relationship between evaluation criteria and influence factors

Factor	RSD of aluminum temperature ( $Y1$ )/%	Melting time ( $Y2$ )/h	RSD of furnace temperature ( $Y3$ )/%
$S$	10.42–4.39 $S$	6.20–1.08 $S$	22.04–1.37 $S$
$\alpha$	16.53–0.080 $\alpha$	19.95–0.36 $\alpha$ + 0.0023 $\alpha^2$	8.17+0.14 $\alpha$
$H$	21.83–0.0091 $H$	4.03+8.2 $E$ –4 $H$	–2.19+0.0086 $H$ –2.43 $E$ –6 $H^2$
$\theta$	5.92+0.17 $\theta$	11.61–0.39 $\theta$	22.94–0.62 $\theta$ +0.025 $\theta^2$
$n$	34.51–44.98 $n$ +19.54 $n^2$	63.73–99.97 $n$ +42.86 $n^2$	22.75–2.30 $n$
$T$	4.98+0.0071 $T$	9.03–0.0063 $T$	19.57–0.0092 $T$ +1.83 $E$ –5 $T^2$
$M$	2.52+0.013 $M$	23.32–0.0062 $M$	19.15–0.026 $M$

## 7 Conclusions

1) By multi-element non-linear regression on the basis of simulation results, the empirical correlations for the RSD of aluminum temperature, melting time and RSD of furnace temperature on the influence factors are obtained as follows:

$$\begin{cases} Y1 = 24.592\theta^{0.296} H^{-2.199} S^{-0.42} \alpha^{-0.8} T^{0.341} \cdot \\ \quad M^{0.743} (n+195.676)^{2.024} \\ Y2 = 88.045\theta^{-0.893} H^{0.284} S^{-1.987} \alpha^{0.971} (\alpha + \\ \quad 0.63n + 32.083)^{0.668} T^{-0.346} M^{-1.286} n^{0.325} \\ Y3 = 8.94\theta^{-0.29} (\theta - 0.113H + 0.207T + 174.003)^{3.401} \cdot \\ \quad H^{3.471} S^{-0.007} \alpha^{0.639} T^{-2.676} M^{-0.184} n^{-151} \end{cases}$$

2) The rules of influence factors on melting process of aluminum melting furnaces are achieved through numerical analysis: 1) RSD of aluminum temperature, RSD of furnace temperature and melting time decrease with swirl number. 2) RSD of aluminum temperature decreases with horizontal angle between burners. RSD of furnace temperature increases with horizontal angle between burners. Melting time, firstly, decreases with horizontal angle between burners, then increases. 3) RSD of aluminum temperature decreases with height of burner. RSD of furnace temperature, firstly, decreases with height of burner, then increases. Melting time increases with height of burner. 4) RSD of aluminum temperature increases with vertical angle of burner. RSD of furnace temperature, firstly, decreases with vertical angle of burner, then increases. Melting time decreases with vertical angle of burner. 5) RSD of aluminum temperature and melting time firstly decrease with mass ratio of air to fuel, then increases. RSD of furnace temperature decreases with mass ratio of air to fuel. 6) RSD of aluminum temperature and RSD of furnace temperature increase with air preheated temperature. Melting time decreases with air preheated temperature. 7) RSD of aluminum temperature increases with natural gas flow. RSD of furnace temperature and melting time decrease with the natural gas flow.

## Acknowledgements

The authors gratefully acknowledge the support of the Changshu Aluminum Industry Co. Ltd. and Suzhou Longray Thermal Technology Co. Ltd., particularly Changshu Aluminum Industry Co. Ltd. for assistance in the running of experimental program.

## References

[1] LI Tian-xiang, HASSAN M, KUWANA K, SAITO K,

VISWANATHAN S, HAN Qing-you, KING P. Thermodynamic analyses of energy utilization and pollutant formation control in secondary aluminum melting furnaces [C]//Proceedings of the Technical Sessions. Warrendale, PA, USA: TMS, 2003: 43–51.

[2] GOLCHERT B, RIDENOUR P, WALKER W, GU M, ZHOU C Q. Effects of nitrogen and oxygen concentration on NO<sub>x</sub> emissions in an aluminum furnace [C]//IMECE2006. Chicago, IL, USA: ASME, 2006.

[3] WILLIAMS E M, STEWART D L, OVERFIELD K. Evaluating aluminum melting furnace transient energy efficiency [C]//Energy Technology Perspectives: Conservation, Carbon Dioxide Reduction and Production from Alternative Sources. Warrendale, PA, USA: TMS, 2009: 181–185.

[4] LAZIC L, VARGA A, KIZEK J. Analysis of combustion characteristics in a aluminium melting furnace [J]. Metalurgija, 2005, 44(3): 195–199.

[5] KUMAR A, VENUTURUMILLI R, KING P E. An investigation of the flame-burden interaction during remelting in an experimental aluminum reverberatory furnace [C]//Extraction and Processing Division—EPD Congress 2008. New Orleans, LA, USA: TMS, 2008: 61–66.

[6] GOLCHERT B, KUMAR A, VENUTURUMILLI R, ADHIYA A, BELT C, TESSANDORI J. How flames/loads interaction affects furnace efficiency in round top furnace operation [C]// 136th TMS Annual Meeting. Orlando, FL, USA: TMS, 2007: 61–66.

[7] KING P E, HATEM J J, GOLCHERT B M. Energy efficient operation of secondary aluminum melting furnaces [C]//9th Annual Electric Utilities Environmental Conference. Tucson, AZ, USA: Electric Utilities Environmental Conference, 2006: 9–14.

[8] BELT C K, GOLCHERT B M, KING P E, PETERSON R D, TESSANDORI J L. Industrial application of doe energy savings technologies to aluminum melting [C]//Light Metals 2006. Warrendale, PA, USA: TMS, 2006: 881–885.

[9] KING P E, HAYES M C, LI T, HAN Q, HASSAN M, GOLCHERT B M. Design and operation of an experimental reverberatory aluminum furnace [C]//Light Metals 2005. Warrendale, PA, USA: TMS, 2005: 899–904.

[10] KING P E, GOLCHERT B M, LI T, HASSAN M, HAN Q. Energy efficient operation of aluminum furnaces [C]//9th Annual Electric Utilities Environmental Conference. Tucson, USA: Albany Research Center, 2005.

[11] BELT C. Energy efficiency tests in aluminum combination melting and holding furnaces [C]//Light Metals 2004. Warrendale, PA, USA: TMS, 2004: 613–617.

[12] LI Tian-xiang, KING P, HASSAN M, KUWANA K, SAITO K. An analytical furnace model for optimizing aluminum melting furnaces [C]//Light Metals 2005. Warrendale, PA, USA: TMS, 2005: 875–879.

[13] PENMETS SA S, TIANXIANG L, KING P, SAITO K. Scale modeling of aluminum melting furnaces [C]//Light Metals 2005. Warrendale, PA, USA: TMS, 2005: 881–886.

[14] NIECKELE A O, NACCACHE M F, GOMES M S P. Numerical modeling of an industrial aluminum melting furnace [J]. Journal of Energy Resources Technology, 2004, 126: 72–81.

[15] NIECKELE A O, NACCACHE M F, GOMES M S P, CARNEIRO J N E, SILVA B G E. Performance of the combustion process inside an aluminum melting furnace with natural gas and liquid fuel [C]// IMECE 2005. Orlando, FL, USA: ASME, 2005: 275–283.

[16] NIECKELE A O, GOMES M S P, NACCACHE M F, MENEZES R C. Influence of the type of oxidant in the combustion of natural gas inside an aluminum melting furnace [C]//IMECE2006. Chicago, IL, USA: ASME, 2006: 1–10.

- [17] NIECKELE A O, GOMES M, NACCACHE M F, KOBAYASHI W T. The influence of oxygen injection configuration in the performance of an aluminum melting furnace [C]//Asme-publications-htd. Fairfield, America: ASME, 1999: 405–412.
- [18] NIECKELE A O, NACCACHE M F, GOMES M S P, KOBAYASHI W T. Numerical investigation of the staged versus non-staged combustion process in an aluminum melting furnace [C]// ASEM Joint Thermophysics and Heat Transfer Conference. Albuquerque, NM, USA: ASME, 1998: 253–260.
- [19] CLARK J A. Secondary aluminum melting research in a laboratory scale reverberatory furnace [C]//Light Metals 2003. Warrendale, PA, USA: TMS, 2003: 769–772.
- [20] STEVENS W, FORTIN J Y. Development of a pilot "top-charge" melt furnace to examine the fundamental melting phenomena in aluminum [C]//Light Metals 2002. Warrendale, PA, USA: TMS, 2002: 747–750.
- [21] LI Shi-xuan, LI Hao. Thermal equilibrium test and energy saving analysis for aluminum smelting furnace [J]. Energy Saving of Non Ferrous Metallurgy, 2009, 25(6): 40–42. (in Chinese)
- [22] YANG Quan. Numerical simulation of metal solidification and casting process [M]. Hangzhou: Zhejiang University Press, 1998: 38–48. (in Chinese)
- [23] ZUO Hai-bin, ZHANG Jian-liang, YANG Tian-jun. Research and application on heat transfer model of hearth including phase-change heat transfer [J]. The Chinese Journal of Process Engineering, 2008, 8(1): 123–129. (in Chinese)
- [24] WANG Ji-min. Numerical simulation and optimization of melting process of a regenerative aluminum melting furnace [D]. Changsha: Central South University, 2012: 21–51. (in Chinese)
- [25] TIAN Rong-zhang. Aluminum casting alloy [M]. Changsha: Central South University Press, 2006: 182–151. (in Chinese)
- [26] ZHANG Zhong-yu. Technique and equipment of aluminum and aluminum alloy [M]. Changsha: Central South University Press, 2006: 37–43. (in Chinese)
- [27] FU Zhi-hua. Thermal process and energy saving of aluminum melting furnace [J]. Energy for Metallurgical Industry, 1987, 5(6): 30–33. (in Chinese)
- [28] ZHOU Jia-rong. Question-answer of melting and casting technology for aluminum alloy [M]. Beijing: Metallurgy Industry Press, 2008: 71–81. (in Chinese)
- [29] LU Yan, LIU Yuan-chao. Measures for increase of heating efficiency and decrease of energy consumption of aluminum smelting furnaces and heat-treating furnaces in the USA [J]. World Nonferrous Metals, 2006, 20(6): 16–19. (in Chinese)

## 烧嘴对蓄热式铝熔炼炉熔炼过程的影响

王计敏<sup>1</sup>, 许朋<sup>1</sup>, 闫红杰<sup>2</sup>, 周子民<sup>2</sup>, 李世轩<sup>3</sup>, 贵广臣<sup>3</sup>, 李文科<sup>1</sup>

1. 安徽工业大学 冶金与资源学院, 马鞍山 243002;
2. 中南大学 能源科学与工程学院, 长沙 410083;
3. 苏州新光热能科技有限公司, 苏州 215008

**摘要:** 结合蓄热式铝熔炼炉熔炼过程的特点, 运用 FLUENT UDF 和 FLUENT Scheme 混合编程, 耦合用户自定义熔化模型和燃烧器换向及燃烧量变化模型, 实现了蓄热式铝熔炼炉熔炼过程的数值模拟。依据优化原则, 获得了熔炼时间随影响因子的变化规律: 熔炼时间随着旋流数、燃烧器倾角、空气预热温度或天然气流量的增加而缩短; 熔炼时间随着燃烧器间水平夹角或空燃比的延长, 先减小而后增加; 熔炼时间随着燃烧器高度的增加而延长。  
**关键词:** 蓄热式铝熔炼炉; 烧嘴; 熔炼过程; 数值模拟; 非线性多元回归

(Edited by Xiang-qun LI)